Journal of Additive Manufacturing Technologies
DOI: 10.18416/JAMTECH.2111594

Infinite Science | Publishing

Investigating compressive strength of laser powder bed fusion manufactured Ti6Al4V lattice structures for bone implant applications

D. Gürkan[1], B. Sagbas[1*]

[1] *Mechanical Engineering Department, Yildiz Techhnical University, İstanbul, Turkey*

[*] *Corresponding author, email: bsagbas@gmail.com*

Abstract

Lattice structures are becoming more and more attractive and preferred structures day by day because of their ultra-light weight properties with specific strength, load bearing capacity and time-cost-material efficiency. Due to their complex geometries it is impossible to generate these structures by conventional manufacturing methods. Laser powder bed fusion (LPBF), one of the most widely used and rapidly developing additive manufacturing (AM) method, provide opportunity to build up complex geometries. Ti6Al4V is commonly used AM material for biomedical lattice structure applications especially for bone implant researches. Mechanical properties of the lattice structures can be altered with lattice parameters (strut diameter, strut shape, unit cell dimensions and orientation). Compressive strength properties are the most critical concern for biomedical lattice structures as they are mostly employed under high compressive load. So, for developing functional, biomedical lattice geometries it is necessary to investigate the compression behavior of different lattice topologies. In this study, octahedral, star and dodecahedron cubic lattice structures were manufactured with Ti6Al4V powder by LPBF technique for investigating their compressive behavior. Young modulus, maximum compression stress, experimental load values are determined and compared with literature. Mechanical properties of lattice structures were evaluated for bone implant applications.

Keywords: Compression test, Lattice structures, Additive manufacturing, Ti6Al4V, Bone implants.

1.Introduction

Lattice structures are consisted a group of unit cells that can be arranged on any axis without gaps among cells. These structures allow building unique topologies which are useful solution for reducing part weight, manufacturing time and absorbing energy, etc [1]. The most specific types of lattice structures can be classified as strut-based and triply periodic minimal surfaces (TPMS). Strut-based lattices are the unit cells with composition of regular set of strut beams linkage within each other. [2]. This study focused on strut-based truss structures.

The advantage of lattice structures is that the possibility of controlling their mechanical properties via different topologies and lattice parameters such as strut diameter/length ratio and unit cell orientation with angular aspect [3]. The fact that complex geometries that are impossible or very difficult to obtain with traditional manufacturing methods, additive manufacturing (AM) is the solution for such industrial applications.

Laser Powder Bed Fusion (LPBF) is a method of AM techniques where a laser beam source melts selectively layers of alloyed metal powder particles building a near net shape part according to 3D CAD model on software [4].

As stated in the literature, Ti6Al4V components manufactured via LPBF are commonly used in biomedical, automotive, aerospace and aviation applications. Titanium alloys are characteristically chosen for these applications because of their biocompatibility, high corrosion resistance and specific strength abilities [5]. Many studies have been focused on biomedical application of Ti6Al4V lattice structure to progress on sophisticated orthopedic implants [6, 7]. Different lattice topologies such as octahedral [8], diamond [9], truncated cuboctahedron [10], gyroid [11], etc. have been used on these studies.

Compressive strength property is one of the most evaluative concerns for LPBF manufactured lattice structures. Many applications of these structures need energy absorption capability and high compressive strength [12]. Bone implant applications require low elastic modulus due to the stress shielding phenomenon [13]. This phenomenon is occurred when the metal implant stiffness is higher than bone tissue and results as bone tissue loss. Using lattice topologies is an effective way to deal with this phenomenon [14]. Therefore, it has great interest to search mechanical properties of Ti6Al4V with different lattice structures for orthopedic applications. Raghavendra et al. [15], performed compression tests on regular, irregular and fully random lattice structures. Arabnejad et al. [16] studied octet and tetrahedron lattice structures with different porosity. Their study showed that the porosity has important effect on mechanical properties. Gangireddy et al. [17] studied octet lattice structures with different strut radius to observe dynamic mechanical responses. Energy absorption capacity and compressive strength value of lattice structures were stated as improved with the square of the strut radius.

It is clear from literature studies that the type and dimensions of the lattice structures highly affect compressive responses of part. However, most of the existing studies do not focus on thin strut diameter structures manufactured by LPBF technology. Optimal lattice type and dimensions have not been reported yet for biomedical applications. Research has been continuing on different lattice topologies and dimensions.

In this study preliminary results of the ongoing research about defining the most suitable lattice structures for orthopedic applications were reported. Star, dodecahedron and octahedral Ti6Al4V lattice structures with thin strut diameter by laser powder bed fusion technology was manufactured for biomedical applications as cubic samples. Compression tests were applied and the results were compared between three lattice structures.

2. Material and methods

Virgin Ti6Al4V powder (EOS, EOS GmbH, Germany) which has a size distribution between 28.14 µm (d10) and 54.84 µm (d90) was used for manufacturing cubic lattice samples. The chemical composition of the Ti6Al4V alloy powder was given in Table 1. Cubic Ti6Al4V lattice samples were manufactured by EOS M280 system (EOS GmbH, Germany). LPBF process parameters were given in Table 2.

Table 1. The chemical composition of Ti6Al4V powder (EOS) [18].

Ti (%)	Al (%)	V (%)	Fe (%)	O (%)	N (%)	C (%)	H (%)	Y (%)
88	6.75	4.5	0.3	0.2	0.05	0.08	0.015	0.005

Table 2. LPBF process parameters.

Laser Power	Scanning Speed	Layer Thickness	Hatch Distance
150 W	1250 mm/s	60 µm	40 µm

Siemens NX version 12.0 (Siemens AG, Germany) was used for design of lattice structures. Star, dodecahedron and octahedral lattice structures were manufactured as 10x10x10 mm like as a compression test samples according to ISO 13314 [19]. 0.25 mm strut diameter and 1.25x1.25x1 mm (xyz) unit cell dimensions were chosen as lattice parameters. All samples were built on z-direction. A 2 mm support structure was added below of part. Orientation of the samples on to the build plate can be seen in Fig. 1a.

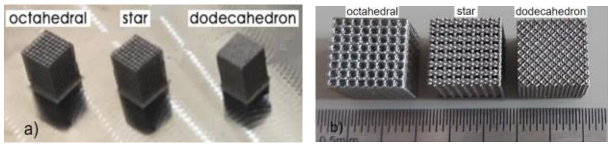

Fig 1. Build orientation of the compression test samples (a), Manufactured cubic lattice samples (b).

Support structures were removed by wire erosion. Top view of the manufactured cubic lattice samples can be seen in Fig. 1b.

Before compression tests, SEM images were taken by Zeiss EVO LS 10 (Zeiss, UK) scanning electron microscope via secondary electron detector with different magnifications for lattice topology observation. Design data, unit cell and SEM image of the pore on manufactured lattice samples can be seen in Fig. 2.

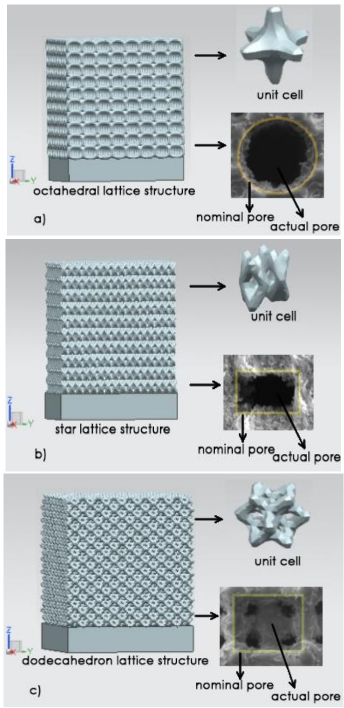

Fig 2. Design of lattice structures: octahedral (a), star (b) and dodecahedron (c) with unit cell and SEM images.

Compression tests were carried out using a calibrated 100 kN universal mechanical tester (Instron 5982, Instron, USA). Test samples were located on the center between two plates. Bottom plate was secured and the top plate was moved with constant strain rate 0.5 mm/min downwardly. Compression tests were performed in the build direction. The tests were repeated three times with the samples which were manufactured in different time period with the same process parameters and average values were reported.

Topology optimization and lattice types control the absolute material distribution for structure and it is important to describe the difference when variable topologies are used. A lightweight structure with high porosity level can be manufactured occupying a specific

DOI: 10.18416/JAMTECH.2111594

volume fraction and it is caused variable results with different lattice topologies [20]. For this, lattice topology volume loss ratios were observed via Siemens NX.

3. Results and discussion

SEM images, taken before compression tests can be seen in Fig. 3. It is clear from the images that partially melted powders remained on the lattice geometry which was because no post cleaning procedure was applied to test samples. More accurate topographical characteristics were obtained on octohedroid lattice topography. Strut diameters were measured as 0.2679 mm, 0.2932mm and 0.2166 mm for octahedral, star and dodecahedron lattice structures respectively. Detailed topographical characterization and dimensional measurements results were reported in the authors' previous study [21].

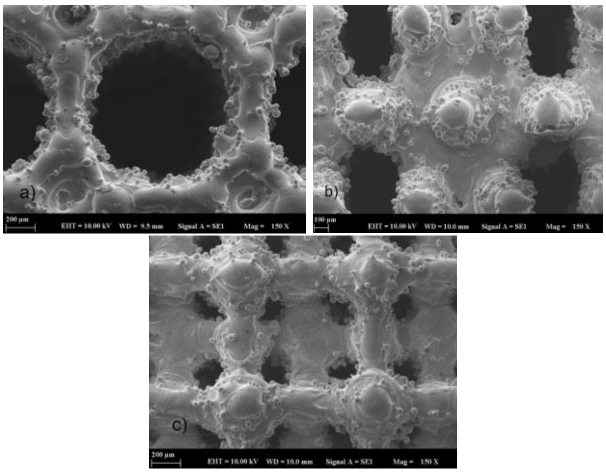

Fig 3. SEM images of octahedral (a), star (b) and dodecahedron (c) lattice structures

Common metal part compressive stress-strain curve is consisted three stages: elastic bending, brittle crushing (plastic plateau) and densification for lattice structures (22). Elastic bending is area of elastic deformation of lattice response to load where the strain energy is kept in the reversible bending of the struts and can be exhibited a linear stress-strain relationship. Brittle crushing is area of yielding point where small increase of stress in load leads additional strain. Densification is area of collapse zone where struts begin to bump into each other [23- 24]. Compressive stress is calculated as applied loading force/effective cross section area. Maximum compressive stress (σ_{max}) is represented the point at which any material can take maximum possible stress at the turning point between elasticity and plateau stage. Compressive strain is calculated as real time displacement of the total length of lattice structure. [25] Typical compression curve for metal lattice structures can be seen in Fig. 4-a.

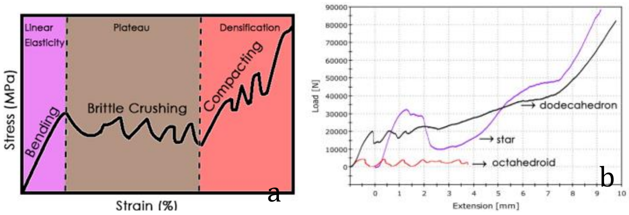

Fig 4. Metal lattice compression curve (a), experimental load-extension diagram (b).

Experimental load and extension curves were shown in Fig. 4-b. The maximum load of octahedral lattice was 4154.41 N while the maximum load of star lattice was 88515.02 N and the maximum load of dodecahedron lattice was 90000.13 N. Compared with dodecahedron and star lattices, the maximum load of the octahedral was found quite low.

Fig. 5 shows compressive stress- compressive strain curves of the lattice samples. Elastic modulus values for octahedral, star and dodecahedron lattices were 1945.74 MPa, 4867.72 MPa and 5897.85 MPa respectively. Young modulus of dodecahedron lattice was 1.2 and 3 times larger than star and octahedral lattices respectively. Young modulus of star lattice was 2.5 times larger than octahedral lattice. Maximum compressive stress was calculated as 38.78 MPa for octahedral lattice while it was calculated as 850.77 MPa and 882.26 MPa for star and dodecahedron lattice structure samples respectively.

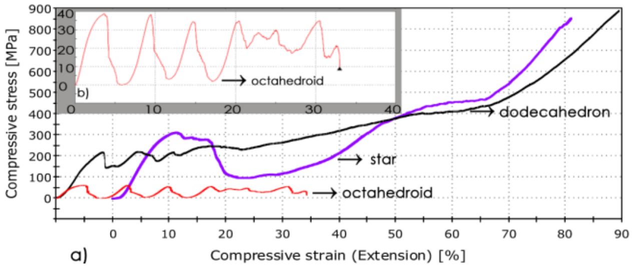

Fig 5. Compressive stress-strain diagram of lattice structures (a) and scaled diagram of octahedral lattice (b).

Different compressive curves were observed for three lattices as shown in above figures with different deformation behaviors. It is clear that different cell types showed different deformation characteristics. For the octahedral lattice structures, there were more concave downward forms on the diagram. Therefore linear elastic part in the stress–strain curve was not completely linear and this situation reduces elastic modulus [26]. Compressive stress increased linearly relative to the strain then it was repeatedly lost and retrieved during the plastic plateau stage which can be seen as multiple peaks (Fig. 6a). Initial collapse of the lattice structure at the former layer occurs and after the load is reallocated to the latter layers beginning to stress regain [27]. Finally planar deformation occurred in the brittle crushing region. The curves of octahedral lattices showed three peaks corresponding to ten units cell layer of octahedral lattices (1.25x1.25x1 unit cell dimension and 10x10x10 lattice structure dimension). Peak values did not change majorly. Small reductions were observed. When octahedral lattices lose one layer, structure maintain own strength and structural integrity until densification stage [28]. This situation caused planar deformation (densification of the piece by splitting it in two) [29]. For the star lattice structures it has been observed an elastic deformation before densification as a slope. Then compressive strength was gradually reduced before densification. It was also observed similar behavior for dodecahedron lattice structures (Fig. 5). During compression tests dodecahedron lattice was showed better mechanical performances than star and octahedral lattice structures.

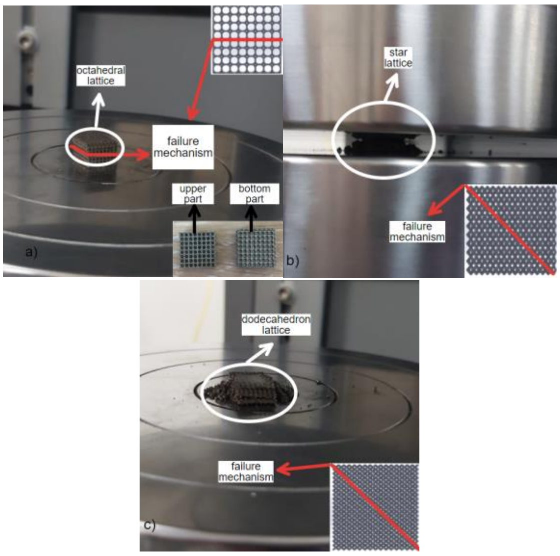

Fig 6. Final form of the samples at the end of the compression tests. Octahedral (a), star (b), dodecahedron (c).

Fig. 6 shows the final form of the samples. Because it was not possible to record the failure mechanisms during the tests, representative drawings on the CAD data were provided to demonstrate the failure mechanism of lattice structures.

It can be seen that layer by layer densification was the main failure mode for octahedral lattice structure due to the planar deformation. Several layers began to absorb the tension during the crushing and after the specific time, the intermediate layer broke and showed this crushing behavior (Fig. 6a). The other two lattice structures were more likely showed orthogonal deformation with tend to crumble in pieces. Unit cell struts started to fall pieces without plastic deformation during compacting and shear deformation occurred in unit cells. This also showed that different lattice structures had own failure mechanism [27, 29- 30].

Dodecahedron lattice caused 63.33% volume loss while octahedral and star lattices caused 83.17% and 53.52% volume loss respectively comparing with 10x10x10 solid cubic samples. The lower compressive strength of the octahedral structure may have been caused by its high volume loss.

Young modulus of Ti alloys are needed to decrease to prevent stress shielding phenomenon for biomedical applications. Typical range of elastic modulus of human bone being are accepted as as 4-30 GPa [31, 32]. Therefore, some studies accepted this range as 1–27 GPa [33]. In this aspect, manufactured structures in this study can be accepted as suitable for biomedical applications.

4. Conclusions

Lattice structures are widely used in biomedical area. In this study, Ti6Al4V lattices were manufactured by LPBF method as octahedral, star and dodecahedron topologies. Deformation of the structures under compression test, SEM analysis and volume loss of lattice topologies were researched. It can be concluded that;

- SEM observation showed that lattice structures were manufactured without defects and compression test could have been implemented.
- During compression tests dodecahedron lattice was showed better mechanical performances than star and octahedral lattices. Latter was star lattice structure. Octahedoid lattice structure performed less mechanical properties than these two lattices.
- Dodecahedron and star lattice structures showed similar elastic deformation behavior and orthogonal failure while octahedral lattice structures showed three peaks until beginning of densification, maintained compressive stress and showed planar failure.
- All the three lattice structures were determined as suitable for biomedical applications in terms of their elastic modulus. Due to the low compressive strength of octahedral lattice structure, it is more likely suitable for cancellous bone applications.
- For the future remarks, research is ongoing with various lattice dimensions for orthopedic applications. Beside tensile and compression tests, microstructural evaluation, biocorrosion and bioactivity tests are ongoing for a comprehensive evaluation.

Acknowledgments

This work was supported by Yildiz Technical University Scientific Research Projects Coordination Unit. Project Number: FDK-2021-4135.

Author's statement

Conflict of interest: Authors state no conflict of interest. Informed consent: Informed consent has been obtained from all individuals included in this study.

References

1. Saremian, R., et al., *Experimental and numerical investigation on lattice structures fabricated by selective laser melting process under quasi-static and dynamic loadings.* The International Journal of Advanced Manufacturing Technology, 2021. 112: p. 2815-2836.
2. Jin, Y., et al., *Design and Characterization of Sheet-Based Gyroid Porous Structures with Bioinspired Functional Gradients.* Materials, 2020. 13(17): 3844.
3. Vilardell, A. M., et al., *Mechanical behavior of in-situ alloyed Ti6Al4V (ELI)-3 at.% Cu lattice structures manufactured by*

DOI: 10.18416/JAMTECH.2111594

laser powder bed fusion and designed for implant applications. Journal of the Mechanical Behavior of Biomedical Materials, 2021. 113: 104130.

4. Scetinec, A., D. Klobcar and D. Bracun, *In-process path replanning and online layer height control through deposition arc current for gas metal arc based additive manufacturing.* Journal of Manufacturing Processes, 2021. 64: p. 1169-1179.
5. Singla, A. K., et al., *Selective laser melting of Ti6Al4V alloy: Process parameters, defects and post-treatments.* Journal of Manufacturing Processes, 2021. 64: p. 161-187.
6. Attarilar, S., et al., *3D Printing technologies in metallic implants: A thematic review on the techniques and procedures.* International Journal of Bioprinting, 2021. 7(1): 306.
7. Mamoud, D., K. S. Al_Rubaie and M. A. Elbestawi, *The influence of selective laser melting defects on the fatigue properties of Ti6Al4V porosity graded gyroids for bone implants.* International Journal of Mechanical Sciences, 2021. 193: 106180.
8. Yan, X., et al., *Mechanical and in vitro study of an isotropic Ti6Al4V lattice structure fabricated using selective laser melting.* Journal of Alloys and Compounds, 2019. 782: p. 209-223.
9. Ahmadi, S. M., et al., *Additively manufactured open-cell porous biomaterials made from six different space-filling unit cells: The mechanical and morphological properties.* Materials, 2015. 8(4): p. 1871-1896.
10. Yavari, S. A., et al., *Relationship between unit cell type and porosity and the fatigue behavior of selective laser melted meta-biomaterials*. Journal of the Mechanical Behavior of Biomedical Materials, 2015. 43: p. 91-100.
11. Yan, C., et al., *Ti–6Al–4V triply periodic minimal surface structures for bone implants fabricated via selective laser melting.* Journal of the Mechanical Behavior of Biomedical Materials, 2015. 51: p. 61-73.
12. Zadpoor, A. A., *Mechanics of additively manufactured biomaterials.* Journal of the Mechanical Behavior of Biomedical Materials, 2017. 70: p. 1-6.
13. Sumner D. R. *Long-term implant fixation and stress-shielding in total hip replacement.* Journal of Biomechanics, 2014. 48(5): p. 797-800.
14. Yi, L., et al., *New Developments of Ti-Based Alloys for Biomedical Applications*. Materials, 2014. 7(3): p. 1709-1800.
15. Raghavendra, S., et al., *Tensile and compression properties of variously arranged porousTi-6Al-4V additively manufactured structures via SLM.* Procedia Structural Integrity, 2018. 13: p. 149-154.
16. Arabnejad, S., et al., *High-strength porous biomaterials for bone replacement: a strategy to assess the interplay between cell morphology, mechanical properties*. Acta Biomaterialia, 2016. 30: p. 345-356.
17. Gangireddy, S. et al., *High strain rate mechanical behavior of Ti-6Al-4V octet lattice structures additively manufactured by selective laser melting (SLM).* Materials Science and Engineering: A, 2019. 745: p. 231-249.
18. EOS, *EOS Titanium Ti64 data sheet.* http://www.eos.info, May 30, 2021.
19. International Organization for Standardization, *ISO 13314 Mechanical testing of metals, ductility testing, compression test for porous and cellular metals.* Reference Number ISO. 13314, 2011. p. 1–7.
20. Xiao, Z., et al., Evaluation of topology-optimized lattice structures manufactured via selective laser melting. Materials & Design, 2018.143: p. 27-37.
21. Gurkan, D. and B. Sagbas, Additively manufactured Ti6Al4V lattice structures for biomedical applications. International Journal of 3D Printing Technologies and Digital Industry, 2021. 5(2): p. 155-163. DOI: 10.46519/ij3dptdi.953315
22. Ge, J., et al., *A detailed analysis on the microstructure and compressive properties of selective laser melted Ti6Al4V lattice structures*. Materials & Design, 2021. 198: 109292.
23. Haidar, S. and Sek, M., *Effects of Production Parameters on Density and Tensile Properties of Aluminium MMC Foam.* International Journal of Advanced in Management, Technology and Engineering Sciences, 2018. 8(3): p. 924-933.
24. Li, D., et al., *Comparison of Mechanical Properties and Energy Absorption of Sheet-Based and Strut-Based Gyroid Cellular Structures with Graded Densities*. Materials, 2019. 12, 2183.
25. Carlton, H. D., *Mapping local deformation behavior in single cell metal lattice structures.* Acta Materialia, 2017. 129: p. 239-250.
26. Gibson, L. J. and M. F. Ashby, *Cellular Solids: Structure and Properties*. Cambridge University Press: Cambridge, UK, 2014.
27. Ge, J., et al., *Microstructural features and compressive properties of SLM Ti6Al4V lattice structures.* Surface and Coatings Technology, 2020. 403: 126419.
28. Yang, K., et al., *Additive manufacturing of Ti-6Al-4V lattice structures with high structural integrity under large compressive deformation*. Journal of Material Science Technology, 2019. 35: p. 303–308.
29. Kas, M. and O. Yilmaz, *Radially graded porous structure design for laser powder bed fusion additive manufacturing of Ti-6Al-4V alloy.* Journal of Materials Processing Technology, 2021. 296: 117186.
30. Jain, H., et al., *Microstructure and high temperature compressive deformation in lightweight open cell titanium foam*. Manufacturing Letters, 2021. 27: p. 67-71.
31. Yu, G., et al., *The select of internal architecture for porous Ti alloy scaffold: A compromise between mechanical properties and permeability.* Materials & Design, 2020. 192: 10875.
32. Katz, J. L., *Anisotropy of Young's modulus of bone*. Nature,1980. 283: p. 106-107.
33. Yan, X., et al., *Mechanical and in vitro study of an isotropic Ti6Al4V lattice structure fabricated using selective laser melting.* Journal of Alloys and Compounds, 2019. 782: p. 209-223.